



HAL
open science

Transition between nucleate and film boiling in rapid transient heating

Shanti Fau, Wladimir Bergez, Catherine Colin

► **To cite this version:**

Shanti Fau, Wladimir Bergez, Catherine Colin. Transition between nucleate and film boiling in rapid transient heating. *Experimental Thermal and Fluid Science*, 2017, 83, pp.118-128. 10.1016/j.expthermflusci.2016.12.012 . hal-01743774

HAL Id: hal-01743774

<https://hal.science/hal-01743774v1>

Submitted on 26 Mar 2018

HAL is a multi-disciplinary open access archive for the deposit and dissemination of scientific research documents, whether they are published or not. The documents may come from teaching and research institutions in France or abroad, or from public or private research centers.

L'archive ouverte pluridisciplinaire **HAL**, est destinée au dépôt et à la diffusion de documents scientifiques de niveau recherche, publiés ou non, émanant des établissements d'enseignement et de recherche français ou étrangers, des laboratoires publics ou privés.






Open Archive TOULOUSE Archive Ouverte (OATAO)

OATAO is an open access repository that collects the work of Toulouse researchers and makes it freely available over the web where possible.

This is an author-deposited version published in : <http://oatao.univ-toulouse.fr/>
Eprints ID : 18403

To link to this article : DOI : 10.1016/j.expthermflusci.2016.12.012
URL : <https://doi.org/10.1016/j.expthermflusci.2016.12.012>

To cite this version : Fau, Shanti  and Bergez, Wladimir  and Colin, Catherine  *Transition between nucleate and film boiling in rapid transient heating*. (2017) *Experimental Thermal and Fluid Science*, vol. 83. pp. 118-128. ISSN 0894-1777

Any correspondence concerning this service should be sent to the repository administrator: staff-oatao@listes-diff.inp-toulouse.fr

Transition between nucleate and film boiling in rapid transient heating

r

S. Fau, W. Bergez*, C. Colin

Institut de Mécanique des Fluides de Toulouse, Université de Toulouse, UMR 5502 CNRS/INPT/UPS, Allée du Professeur Camille Soula, 31400 Toulouse, France

A B S T R A C T

This article presents an experimental study of rapid transient boiling regimes of distilled water at saturation on a thin tungsten wire of 50 μm diameter. The heating rate varied from ~ 0.5 to 5×10^5 K/s. Heat supply was obtained by periodic pulses of constant voltage with a period large enough to avoid response overlap. Rapid video recording (14,000 fps) was associated with electrical measurements. Two transient phenomena were studied: pulse heating and thermal relaxation. During pulse heating, it was observed that, depending on heating rate, three kinds of behavior exist: (i) only nucleate boiling appears for small heating rates ($\lesssim 10^5$ K/s), (ii) transition from nucleate boiling to film boiling by bubble coalescence at intermediate heating rates ($\lesssim 2 \cdot 10^5$ K/s), and (iii), at higher heating rates, transition to film boiling by vapor wave propagation (speed ~ 20 m/s). This last mechanism is interpreted as homogeneous nucleation process and is qualitatively similar to an autowave process. In the relaxation stage, it is observed that film collapse is characterized by two mechanisms: film break up into nucleate boiling regime or continuous vapor receding. This second mechanism is compared to a conduction model of a temperature traveling wave in the wire. The time variation of the vapor film length predicted by the model is in the range of the experimental data.

Keywords:
Transient boiling
Critical heat flux
Film boiling
Nucleation
Rewetting

1. Introduction

Boiling heat transfer is widely encountered in industrial and energy processes. It is generally considered as a benefit, as it leads to much higher heat transfer coefficient than in case of single-phase; its main drawback concerns what is called the boiling crisis, as it can lead to severe damages in heat exchangers. Abundant literature exists concerning the case of steady boiling conditions. Transient boiling conditions have been less studied although it exhibits significant differences compared to steady boiling. A number of issues concerning nuclear safety or metallurgy process require a full knowledge and understanding of this boiling configuration.

Some studies on transient boiling were performed at moderate heating rates on flat plate or cylinders [1,2]. Auracher and Marquardt [1] investigate the entire boiling curve from nucleate boiling to critical heat flux and film boiling, and also the rewetting process for a small flat horizontal heated surface. These experiments were carried out with a controlled heating rate up to 50 K/s and showed an increase in the heat transfer coefficient with the heating rate for all the boiling regimes. Recently, Visentini et al. [2] studied the mechanisms of heat transfer during a sudden

power excursion in a vertical semi-annular geometry in pool and flow boiling for heating rate from 1 to 2000 K/s. At small and moderate heating rate, the full boiling curve was observed, with a nucleate boiling regime, CHF and transition to film boiling. An increase of the heat transfer coefficient with the heating rate was also found for all the regimes. The results also showed that the effect of pulse shape was playing a role: for a triangular power signal at heating rate smaller than 5 K/s CHF was well predicted by Katto and Ohno correlation [3], whereas for square power signals and heating rate between 5 and 11 K/s CHF significantly increased and was well predicted by Sakurai et al. model [4]. At higher heating rate around 1000 K/s, explosive boiling is observed and the onset of nucleate boiling was immediately followed by the film boiling regime. Transient boiling has also been studied intensively in the frame of the homogeneous nucleation theory with the technique of wire ultra-fast heating proposed by Skripov [5–9]. In these studies, heating systems were small (thin wire) and heating rate was as large as possible ($\sim 10^6$ K/s). Finally, transition boiling occurs also in quenching experiments and vapor explosions [10]. This case can be considered as a relaxation process with an initial state far from equilibrium. Actually, all these phenomena are also related to a crucial parameter in phase change, the Minimum Heat Flux (MHF) temperature or Leidenfrost temperature. Bernardin and Mudawar [11] have shown that, defining it as a thermodynamic limit (spinodal as well as kinetic), is a simplification that deviates

* Corresponding author.

E-mail address: wladimir.bergez@imft.fr (W. Bergez).

somehow from measurements. In case of transient boiling, the situation seems more complicated, and Bakhru and Lienhard found that the MHF vanishes for small cylindrical heaters (one hundredth of capillary scale) [12]. They proposed a propagation mechanism for film boiling transition, where the Leidenfrost temperature was an intrinsic parameter controlling a transition from nucleate to film boiling without a step change in heat transfer. The same mechanism was formulated later in a more general form by Zukhov and al. [13] as an autowave instability [14].

The aim of this paper is to investigate the case of intermediate heating rate, between purely homogeneous nucleation experiments ($\sim 10^6$ K/s), and “slow” transient experiments ($\sim 10^3$ K/s), in order to characterize the different boiling regimes occurring in this range of heating rates that corresponds to the transition from purely heterogeneous nucleation to purely homogeneous nucleation. By using pulse heating, it was also possible to characterize the relaxation heat transfer when heat supply is switched off. This phenomenon is directly related to rewetting process. The article is organized as follows. In the second section, we introduce the experimental set-up. In the third section, we present, first, the results for the heating phase and we discuss them. Then, we focus on the relaxation stage, and we propose a nonlinear conduction mechanism (autowave) to model the rewetting process by vapor receding, and we compare it to experimental data.

2. Material and method

The experimental apparatus consisted of a small boiling cell ($0.1 \times 0.1 \times 0.1$ m³) with glass walls (Fig. 1). The liquid used was distilled water at atmospheric pressure. Temperature control of the liquid was realized with a heating plate and an auxiliary heater driven by a Pt100 probe through a PID controller and a rotating magnet to homogenize the liquid temperature. The rotating magnet was switched off before each measurement. Few minutes were necessary for the swirl to be attenuated. The possible residual flow was found negligible. All the experiments were done close to saturation temperature. The heating device was made of a thin tungsten wire manufactured by Goodfellow Inc. (25 μ m in diameter and 11 mm length). It was clipped on each end on two mini plastic terminal blocks connected with two copper wires large enough to avoid Joule heating. This system was electrically supplied with a DC voltage controlled by a pulse generator with a power transistor MOSFET. The switching time of the pulse generator was 50 ns, which is negligible compared to the pulse length.

In order to study the boiling relaxation, a resistor was put in parallel with the pulse generator, so that a small electrical current

was supplied to the wire between pulses. The wire voltage, U , and the electrical current intensity, I , were measured through a 14-bit 400 kHz data acquisition system PCI-703. The pulses were of few ms with a period of some tens of ms, large enough to avoid overlap effects between successive pulses. The spatial average temperature of the tungsten wire was obtained by measuring its electrical resistance. A calibration curve was established before and after each test between room temperature and saturation temperature to obtain the linear coefficient of the temperature vs. electrical resistance law. The deviation from linearity of the electrical resistivity dependence with temperature was estimated from [15]; the relative error due to this non-linearity was found to be less than 4% at 1500 K, and was thus neglected. The contributions of the tungsten wire and of the connections and copper wire to the total electrical resistance, were treated differently by assuming that only the temperature of the wire varied when the others remained at liquid temperature. With this assumptions, for an electrical DC current intensity, I , of 1 A, the electrical measurements uncertainties lead to a maximum temperature uncertainty of 2 K, and this error could be neglected.

Only a small fraction of the realized tests could be processed due to tungsten wire burnout in the course of the experiment. This problem was however limited by controlling the voltage supply. This method is different from what is generally done. Indeed, in controlled boiling system, generally either the wire temperature or the heat supply is controlled. The advantage of the first solution is the possibility to explore the whole boiling curve in quasi-static conditions, in particular the transition boiling regime which is naturally unstable. However it is quite uneasy to both control temperature and make rapid transient. For transient experiments, the second method, heat supply control, is generally preferred. However, when power supply increases, because the balance between heat supply and heat transfer to the fluid is largely violated, time transient must be reduced to very short values to avoid burnout. This difficulty was circumvented by controlling the voltage instead of the power supply. A clear advantage of this method is to lead to a passively controlled system, as the electrical current varies oppositely with the temperature. In this manner, it was possible to maintain film boiling up to large temperature without burnout.

Visualizations of the boiling phenomenon during pulses were realized with a rapid video camera (Vision Research Phantom V1210) working at 14,000 fps. The spatial resolution of the images was 119 px/mm (0.0084 mm/px).

For each test, after calibration of the wire resistance with the bath temperature, a period of vigorous boiling obtained with the auxiliary heater was imposed to the liquid during few minutes in order to degas the water. Then pulsed voltage of various length

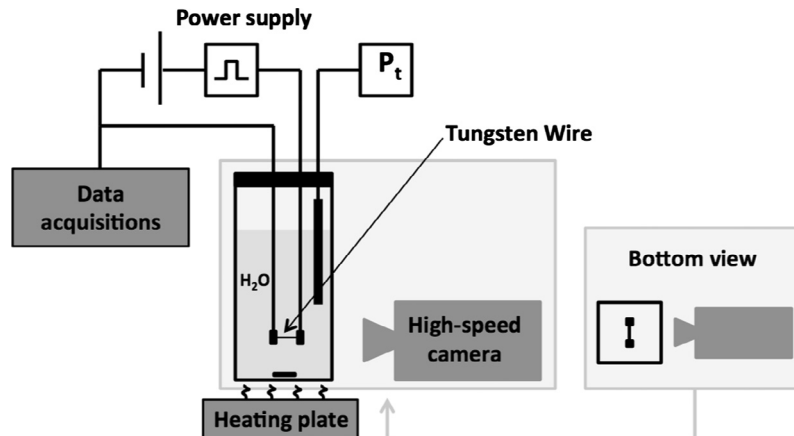


Fig. 1. Schematic diagram of the experimental setup.

and periods were supplied to the tungsten wire, and video recording of the boiling phenomenon were simultaneously performed.

It was observed that, during a train of pulses, the reproducibility of the different quantities of interest was very good. It was then possible to remove the electronic noise by averaging the response to successive pulses. The uncertainties in U and I measurements at the start of the pulse can lead to large error in the first value of the heating rate (K/s); to avoid this problem, we fixed it by an energy balance at $t = 0$, i.e. by equating the rate of wire enthalpy variation at $t = 0$ with the electrical power. It may also be noted that a small variation of the voltage in the pulse (some percent of the initial value) could happen at high energy inputs due to the impedance loss of the transistor. In the relaxation period, the electronic noise was much larger and filtering the signals before post-processing was necessary.

From the measurements of I and U , filtered and averaged over a set of several pulses, we obtained the average response of the temperature to a pulse as a function of time, $T_w(t)$ (Fig. 2). All the results presented in this article are based on such averaged data. It was found that the maximum relative variation in wire superheat between successive pulses was less than 12% for all tests, and even less than 2% for tests 9 and 10. If the error due to nonlinearity in the relation between electrical resistivity and tungsten temperature is taken into account, the maximum relative uncertainty of wire temperature measurements is around 15%. Through an energy balance in the wire, the average heat flux was then estimated as

$$q''(t) = \frac{\sigma(T_w)U^2D}{4L^2} - \rho c(T_w)\frac{D}{4}\frac{dT_w}{dt}, \quad (1)$$

where σ is the electrical conductivity of tungsten, D and L are the wire diameter and length, ρ and c are the tungsten density and heat capacity. The time scale of temperature variation was much larger than the acquisition time, except at the beginning of the pulse. By correcting the initial variation as mentioned above, it was thus possible to neglect temporal uncertainties on the measurements of temperature and its rate of variations. It can be noted that the variation of heat capacity between 300 and 1500 K is approximately 20% (see for instance [16]). It can also be checked that the diffusion length in the tungsten during one pulse is of order 0.5 mm which indicates that heat transfer at the two ends of the wire is negligible. In case of relaxation, Eq. (1) is still valid with $U = 0$. Next, from the video recordings, the different boiling regimes and transitions were identified. In the relaxation phase, basic image processing was used

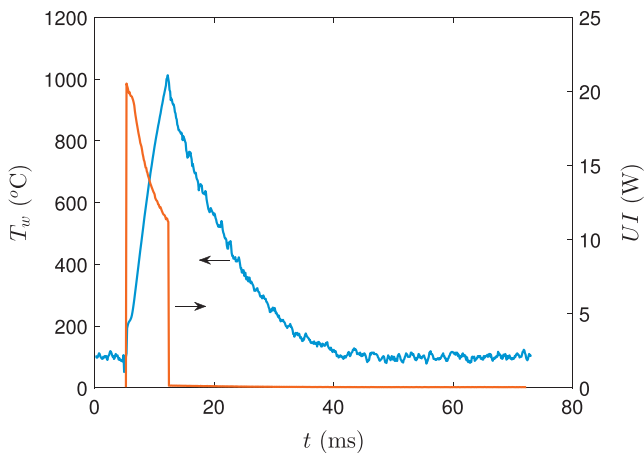


Fig. 2. Average response of wire temperature to a pulse and corresponding power supply (test 8).

to characterize the film collapse in the transition between film boiling and natural convection.

3. Results and discussion

3.1. Heating phase

The different tests processed for the present paper are listed in Table 1. They all correspond to a 7 ms pulse, with a period of 70 ms. T_b is the liquid bulk temperature and is also considered as the initial temperature of the wire, T_{max} is the maximum temperature reached during the test, and q''_{max} is the maximum heat flux. $(dT/dt)_0$ is the initial value of the heating rate corresponding to Joule effect, i.e. heat supply conversion into sensible heat; it is also the maximum value of the heating rate.

The transient boiling curves corresponding to the tests 2–10 are presented in Fig. 3 where the wire superheat is defined as $\Delta T_w = T_w - T_{sat}$. For comparison, we have also plotted experimental data in case of steady boiling (i.e. long pulse for which the wire temperature reaches a stable average value); the curve (a) is a “standard” (steady) boiling curve obtained from two classical correlations, (i) Rohsenow’s for nucleate boiling [17], and (ii), Bromley’s [18] for film boiling; the transition boiling is obtained as a linear interpolation between Critical Heat Flux (CHF) according to [19] and the Minimum Heat Flux (MHF). MHF is here defined as the thermodynamic limit of superheat; it can be approximated as 27/32 of critical temperature for pressures well below the critical point and for Van der Waals state equation [20], i.e. $T_{MHF} \approx 545$ K for water (alternatively, based on Peng-Robinson equation of state, Adevisan computed the kinetic limit of liquid superheat as $T_k = 575$ K at atmospheric pressure). We found that, in steady boiling, the heat flux measured is smaller than the one predicted by Rohsenow’s correlation; this deviation can be attributed to the small value of the Bond number based on wire diameter ($\sim 10^{-4}$). Indeed, as the wire diameter is much smaller than the capillary length of water, smaller bubbles are expected than in larger systems, and consequently latent heat contribution might also be less important; furthermore, because the nucleation site distribution on the wire surface is reasonably thinner than for a standard machined surface as used generally in boiling experiments, nucleation wall superheat tends naturally to be higher, and the active site density smaller.

In case of transient boiling, experimental studies have already shown that the heat flux is an order of magnitude larger than for steady boiling [1,21]. We have found the same tendency (Fig. 3). For tests 2 and 3, the length of the pulse was too short to observe significant variations of q'' and ΔT_w . From tests 6–10, the boiling curves exhibit a well-defined maximum for the heat flux. Beyond this maximum, at large wire superheat, the boiling curves converge towards a common curve for all these tests, i.e. that is independent of the input voltage (Fig. 3). The maximum heat flux should not be assimilated with the standard CHF found in steady boiling. We can observe that it increases with the input voltage, i.e. with the heating rate, a result already reported [21]. But it happens at much larger wall superheat than in the case of a standard boiling experiment, which suggests different mechanisms. We note also that the average wire temperature at maximum heat flux, corresponds to value smaller than the kinetic limit, which suggests that, in the present experiments, nucleation is not strictly homogeneous, if not at all homogeneous, depending on the input voltage. Indeed, an order of magnitude higher in the heating rate, is needed to start plain homogeneous nucleation according to [5]. Tests 4 and 5 do not exhibit a clear maximum heat flux as tests 6–10.

Fig. 4 presents the same results as in Fig. 3, but with the heat transfer coefficient, h , instead of q'' as a function of wire superheat,

Table 1
Tests conditions.

Test number	2	3	4	5	6	7	8	9	10
T_b (°C)	97.3	97.3	97	96.5	98	98	98	98	98
U (V)	1.37	2.07	2.85	3.22	4.04	4.72	5.24	6.27	7.30
T_{max} (°C)	153	175	221	230	529	808	959	1267	1617
q''_{max} (MW/m ²)	1.24	2.76	4.75	5.95	7.85	9.50	10.3	12.8	14.3
$(dT/dt)_0$ (10 ³ K/s)	0.38	0.84	1.47	1.86	2.05	2.76	3.28	4.26	5.52

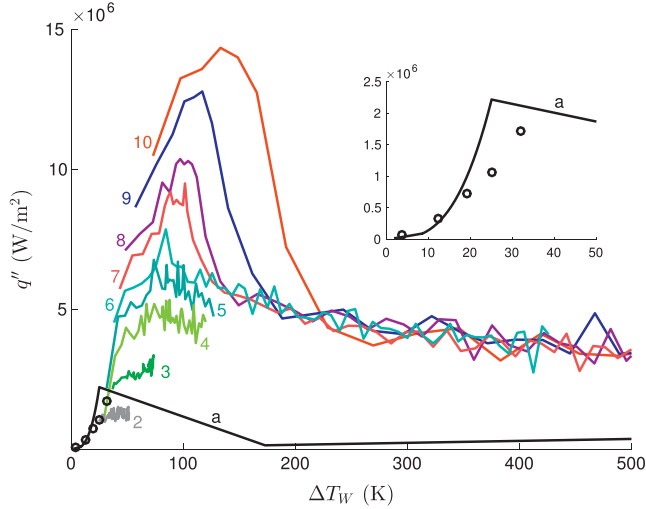


Fig. 3. Boiling curves: heat flux density, q'' , vs. wire superheat ΔT_W ; numbers refer to tests; \circ : steady boiling experiment; (a): standard boiling curve as defined in the text (inset: detail of steady boiling curve).

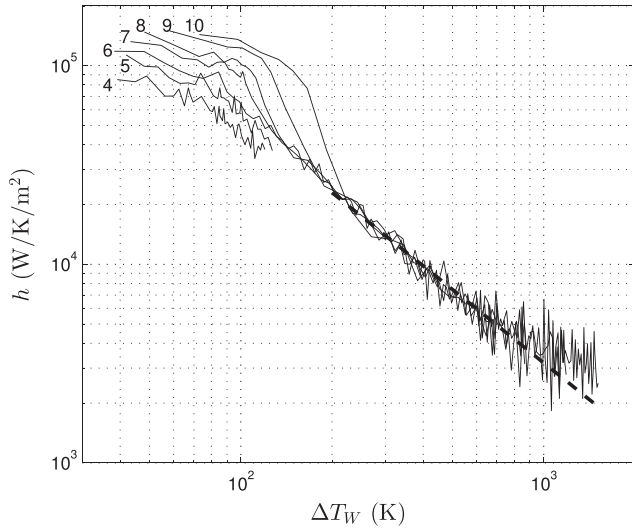


Fig. 4. Heat transfer coefficient, h , vs. wire superheat, ΔT_W ; numbers refer to tests 4–10; broken line represents $h \propto \Delta T_W^{-1.23}$.

ΔT_W . For all the test conditions studied (except 2 and 3), the heat transfer coefficient in boiling regime is a decreasing function of wire superheat. Moreover, the data for test 6 to 10 converge on a unique curve, as ΔT_W increases beyond the maximum heat flux. In this regime, for wire superheat lesser than ~ 700 K, $h \propto \Delta T_W^n$ with $n \approx -1.25$. For higher values of wire superheat, the heat transfer coefficient starts to deviate from this law; this deviation can be interpreted as convergence towards a stationary boiling regime (but analysis of the characteristic time for settling steady

boiling condition has not been done in this study). We note also that, at the maximum heat flux, the heat transfer coefficient increases with the heating rate.

Detailed variations of the wire temperature are shown for test 4, 6 and 10 on Fig. 5. As U is increased, we observe two different behaviors: for test 10, the temperature variations remain monotonous, whereas for test 4, the temperature passes through two local extrema. Test 6 is at the limit between these two behaviors. The presence of two extrema indicates change in heat transfer efficiency. At the first local maximum, the heat transfer to the fluid has increased enough to overbalance the heat supply. This is the signature of the nucleate boiling regime. Then, the presence of a minimum temperature indicates that the heat transfer decreases at some point, a proper effect of transition to film boiling. Indeed, as the video recordings show, in case of low power input (test 2–5), the heat transfer regimes are nucleate boiling followed by partial film boiling (Fig. 7, test 4). When the power supply is increased further (tests 6–10), the nucleate boiling regime shrinks to the appearance of just some bubbles before film boiling spreads over the entire wire. In this case, the heat transfer drops suddenly and the heating rate increases abruptly (local peak). After this transition, the heating rate decreases as a direct consequence of the increase of heat flux with temperature in film boiling and the decrease of heat supply due to the increase of the electrical resistance of the wire. At the intermediate power supply (test 6), the transition to film boiling occurs just when the nucleate boiling regime counterbalances the heat supply (approximately zero heating rate).

The transition to film boiling is characterized by a change of slope of $T(t)$. Fig. 6 details the temporal variations of the wire superheat, $\Delta T_W(t)$, at the start of the pulse for tests 7–10. It compares the experimental curves with the solution of transient heat conduction equation in the wire and the surrounding liquid water. The maximum heating rate corresponding to zero heat transfer to the fluid is also plotted. The figure shows that, in the first instants, the temperature evolution can be approximated by the pure conduction model. A significant deviation from pure conduction occurs soon that can be attributed to the onset of natural convection and to bubbles formation, i.e. an improvement in heat transfer (tests 7–9). The sudden change in slope is then due to the appearance of film boiling. In case of test 10, this transition is directly obtained from pure conduction to film boiling, without a convective phase. This is confirmed by video recording (Figs. 9, 10).

The average wire temperature at which this transition occurs varies with the input voltage as shown by Fig. 6. For test 10, it is found to be close to T_{MHF} as defined above. But, for tests 7–9 it is well below this value. However, it can be observed on Fig. 6 that the transition occurs at approximately the same value of the upper limit of wire superheat (points A in the graphs). This limit corresponds to the case of zero heat transfer to water, i.e. dry wire with perfect insulating vapor; point A was then determined by the change of slope in the derivative of $T_W(t)$ occurring at the transition to film boiling; it is respectively for tests 7–10, $\Delta T_W = 420, 423, 374$ and 419 K. This superheat measures the energy input to have transition to film boiling. From the heat balance Eq. (1) where q'' is set to zero, the corresponding limit superheat is equal to $\frac{4UIt_0}{\pi\rho cD^2L}$,

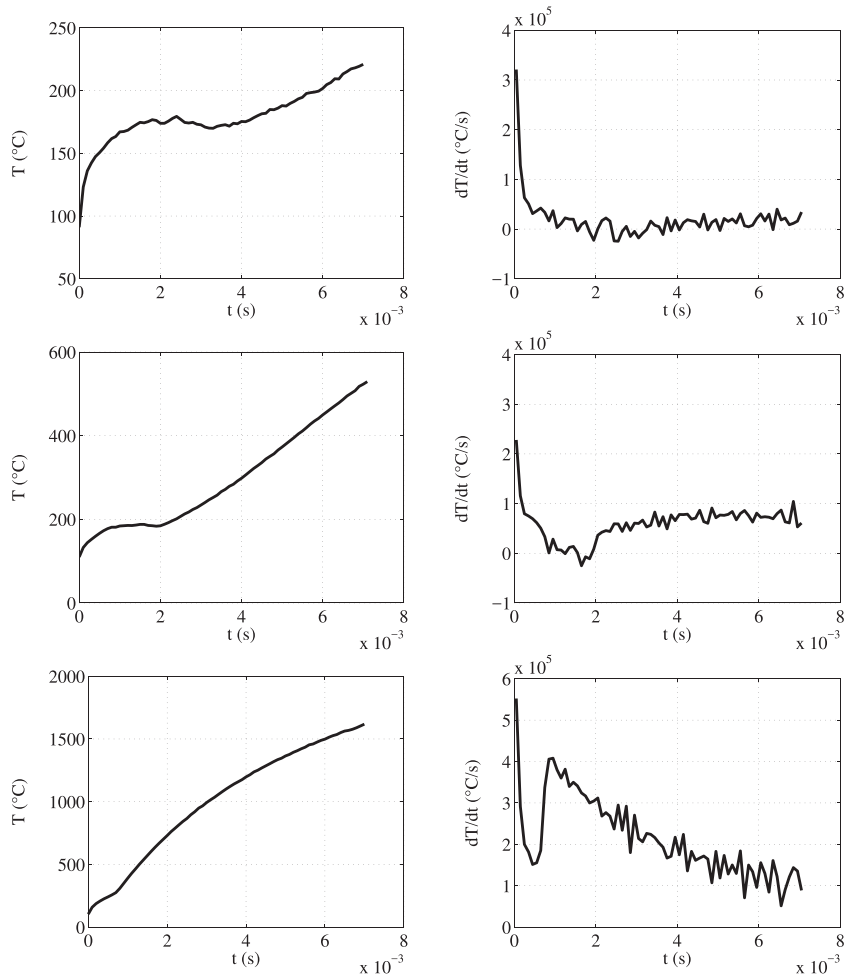


Fig. 5. Wire temperature (left) and heating rate (right) evolutions during a pulse; from top to bottom: test 4, test 6, test 10.

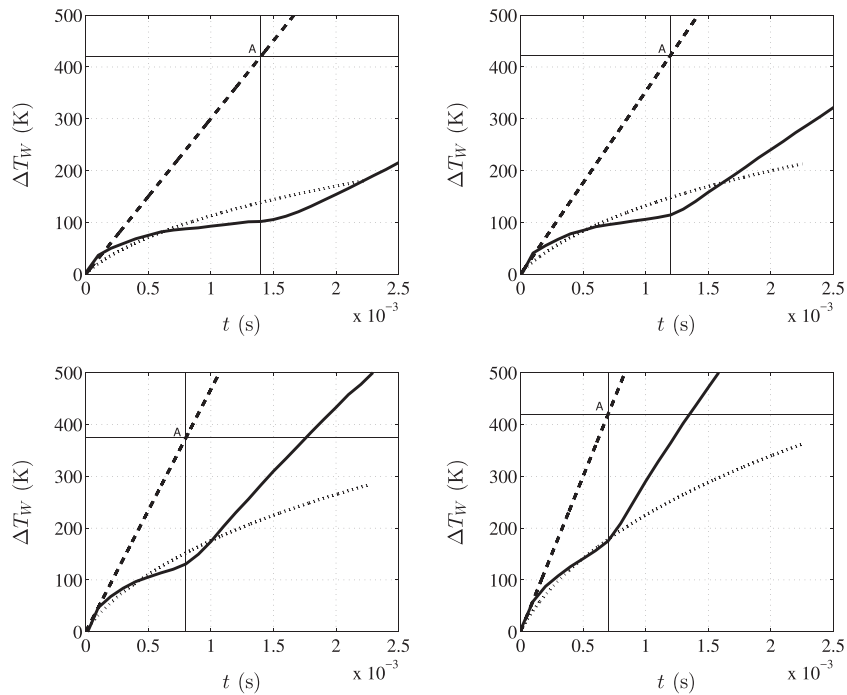


Fig. 6. Initial variations of wire superheat; from left to right and top to bottom: test 7, 8, 9 and 10; solid line: experimental data; broken line: maximum heating rate (zero heat transfer to water); dotted line: solution of transient conduction equation.

where t_0 is the instant of transition. This expression can be put as a function of the electrical current density in the wire, j , as $(\rho c)^{-1} \sigma j^2 t_0$. We found then that the sudden transition to film boiling occurs when the product $j^2 t$ for a given material becomes, at $t = t_0$, larger than a certain value, but also if, in addition, t_0 is lesser than a certain t_m : in our experimental conditions, $t_m \approx 1.5$ ms as test 7 is the first test conducting to this transition (Fig. 6). This condition can be understood in the frame of the homogeneous nucleation process. Indeed, if a bubble grows on a certain location on the wire during the first instant of heating (heterogeneous nucleation), at this location the wire is suddenly embedded in vapor, and the boundary condition for heat conduction in the wire falls down to adiabatic condition; if the heat supply is fast enough, the wire temperature can increase locally and reach a destabilizing value leading spontaneously to homogeneous nucleation. In this process, the energy is the same whatever the heating rate, as long as the initiating bubble remains attach to the wire, i.e. bubble cycle has not the time to establish.

Photographs extracted from the video recordings and corresponding to the tests 4, 6, 8 and 10 of Table 1 are given in Figs. 7–10. For test 4, the photographs cover the entire heating period and the beginning of the relaxation period. The boiling regime is a juxtaposition of nucleate and film boiling depending on the position on the wire. The largest bubbles are of order 0.5 mm, which is well below the capillary length. Film boiling seems to appear by a mechanism of bubble coalescence as it may happen in large boiling systems. This mixed regime leads to heat flux fluctuations observed in the boiling curve, Fig. 3. Similar behavior is observed for test 5 and 6. For test 8, the characteristic features of the boiling regime are strikingly different, although the heating rate has not changed drastically (around 30%). Here, after nucleate boiling has developed for a short period, an isolated bubble grows larger than the other (~ 1 mm) and leads to a sudden or explosive vapor growth by propagation along the tungsten wire with a velocity ~ 20 m/s. It was observed that this velocity exhibits no clear dependency on the input voltage (tests 7–10). Similar structures have already been observed by Zhukov et al. [13] and were interpreted as nonlinear traveling wave driven by the wire superheat. It is noteworthy to see that this mechanism of transition to film boiling is totally different from the coalescence mechanism. It does not need that the system passes through a nucleate boiling regime. After the unstable growth of the vapor film, the wire is completely covered by vapor and its temperature start to grow to high values. Test 6 appears actually as a limit of ‘classical’ CHF when tests 2–5 do not lead to total film boiling, but rather to a kind of transition boiling regime. Finally test 10 exhibits a direct transition to film boiling without any stage of partial nucleate boiling. It is the same mechanism as in test 8, except that the phenomenon starts almost as soon as power is supplied.

The results obtained from the video recordings are in qualitative agreement with the interpretation given on the basis of the

electrical measurements. However, it seems difficult to predict quantitatively, on the basis of a mechanistic model, the transition from “standard” CHF, i.e. limit of nucleate boiling by vapor coalescence, to high heating rate CHF, i.e. appearance of a vapor wave along the wire (homogeneous nucleation process). Even the characterization of this last process through an autowave seems difficult: in case of rapid transient heating, this process is strongly unsteady and far from equilibrium, thus leading to local unknown transient heat transfer coefficients.

3.2. Thermal relaxation

At the end of the pulse heating, a relaxation phase follows (Fig. 2). The time evolution of the average wire temperature is shown for tests 2–10 in Fig. 11. The slope of the curve $\ln(\Delta T_w)$ vs. t is proportional to the heat transfer coefficient. For tests 2–5, the relaxation corresponds mainly to nucleate boiling followed by natural convection. For tests 6–10, it is observed that, initially, the heat transfer coefficient is approximately constant, and, after a certain time, starts to increase. The photographs of the relaxation stage in Fig. 12 show that, for tests 6–8, the heat transfer mechanism is a combination of film boiling on the dry part of the wire, and of natural convection on its wetted part. The deviation of the heat transfer coefficient from a constant value seems to occur when the contribution of natural convection starts to dominate. Test 10 shows that as long as the vapor film remains stable all over the wire, the heat transfer coefficient remains approximately constant. This suggest that it is possible to introduce the characteristic time of an exponential relaxation based on the initial film boiling heat transfer coefficient, $t_c = \rho c d / 4h$. The evolution of t_c vs. initial average wire superheat, $\Delta T_0 = T_0 - T_{sat}$, where T_0 is the maximum temperature reached by the wire is given on Fig. 13 for tests 2–10. Data can be split into two sets: one corresponding to $\Delta T_0 < 250$ K, tests 2–5, and the other to $\Delta T_0 > 400$ K, tests 6–10. Correlations for film boiling heat transfer gives, at first order and with constant thermal properties, power laws, as for instance $h \propto (T_w - T_{sat})^{-n}$ with $n = 0.25$ for [18]. However, due to the large variations of vapor temperature with heat flux, the temperature dependencies of the physical properties of the vapor play a significant role. For instance, the predicted heat transfer coefficient by Bromley correlation is actually approximately independent of wall superheat, at least up to 1000 K of superheat. In the present study, heat transfer coefficient decreases after the maximum heat flux. Thus, for test 10, the heat transfer coefficient at the end of the pulse is about $3.5 \text{ kW m}^{-2} \text{ K}^{-1}$, when for test 6, it is approximately $10 \text{ kW m}^{-2} \text{ K}^{-1}$. A linear regression of t_c with ΔT_0 for test 6–10 data of Fig. 13 ($\Delta T_0 > 400$ K) gives

$$t_c \propto \Delta T_0^n, \quad n = 0.39 \quad (2)$$

which means $h \propto (T_w - T_{sat})^{-0.39}$. It may be noticed that the boiling regime on the wire is generally heterogeneous (simultaneous

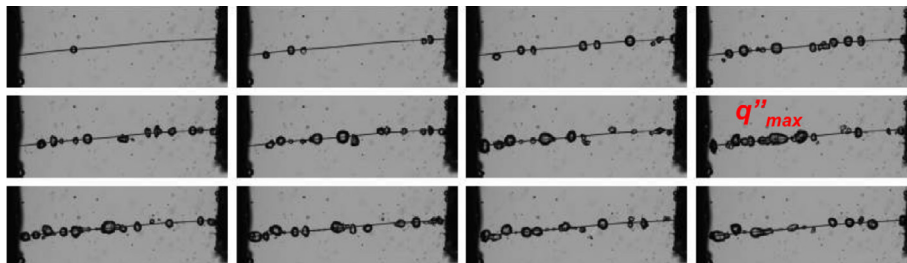


Fig. 7. Onset of boiling: test 4; $\Delta t = 357.05 \mu\text{s}$ between 2 images; wire length: 11 mm; time increases from left to right, top to bottom; label q''_{max} corresponds to image closest to maximum heat flux.

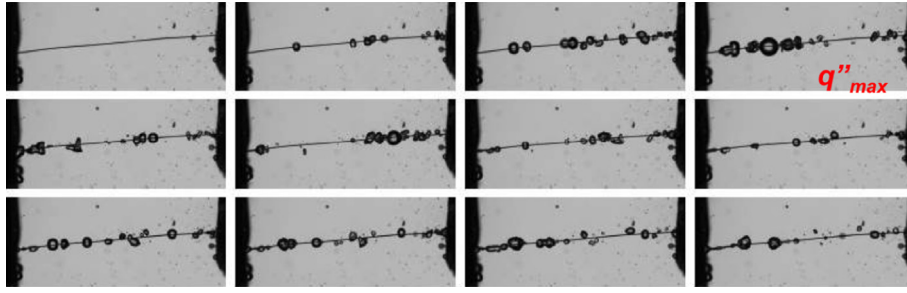


Fig. 8. Onset of boiling: test 6; $\Delta t = 428.46 \mu\text{s}$ between 2 images; wire length: 11 mm; time increases from left to right, top to bottom; label q''_{max} corresponds to image closest to maximum heat flux.

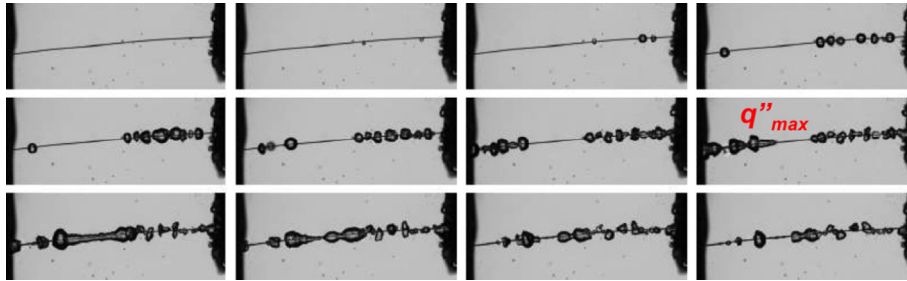


Fig. 9. Onset of boiling: test 8; $\Delta t = 142.82 \mu\text{s}$ between 2 images; wire length: 11 mm; time increases from left to right, top to bottom; label q''_{max} corresponds to image closest to maximum heat flux.

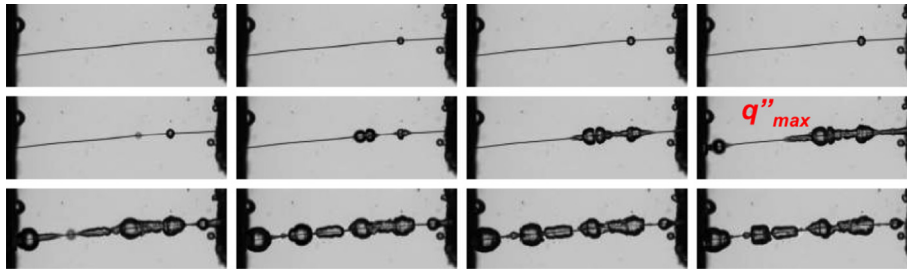


Fig. 10. Onset of boiling: test 10; $\Delta t = 71.41 \mu\text{s}$ between 2 images; wire length: 11 mm; time increases from left to right, top to bottom; label q''_{max} corresponds to image closest to maximum heat flux.

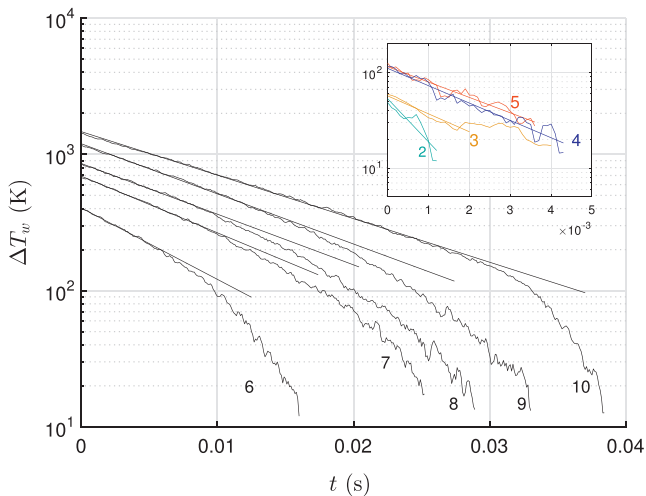


Fig. 11. Time evolution of wire superheat during relaxation. Numbers refer to tests 2–10. Linear lines correspond to exponential relaxation approximation.

occurrences of nucleate and film boiling in distinct zones of the wire), which means also wire temperature heterogeneities. All this may explain the difference between available correlations such as [18] where a homogeneous regime takes place, and rapid transient boiling where the heat transfer rates can vary significantly from one position to another before relaxing towards a steady regime. Finally, we observe also that the spatial average heat transfer coefficient varies by a factor ~ 4 for the 2 sets of data (high temperature, i.e. tests 6–10, and low temperature, i.e. tests 2–5). For $\Delta T_0 > 400 \text{ K}$ (tests 6–10), the heat transfer coefficient is $\sim 2.5\text{--}4 \times 10^3 \text{ W/m}^2/\text{K}$, and for $\Delta T_0 < 250 \text{ K}$ (tests 2–5), it is $\sim 1\text{--}2 \times 10^4 \text{ W/m}^2/\text{K}$. For tests 2–5, video show that boiling ceases quite as soon as pulse ends. It is also interesting to note that, for the same wire superheat, the heat transfer coefficient in relaxation phase is smaller than during rapid heating, which makes clear that heat transfer mechanisms differ quite significantly in both processes.

During relaxation, the heat transfer mode follows an evolution from film boiling to single-phase free convection. From video recordings, we observe as in [22] two different mechanisms of film collapse and rewetting (Fig. 14). In the majority of cases, the film breaks up suddenly all along its length in small bubbles leading to a very short phase of nucleate boiling regime followed by

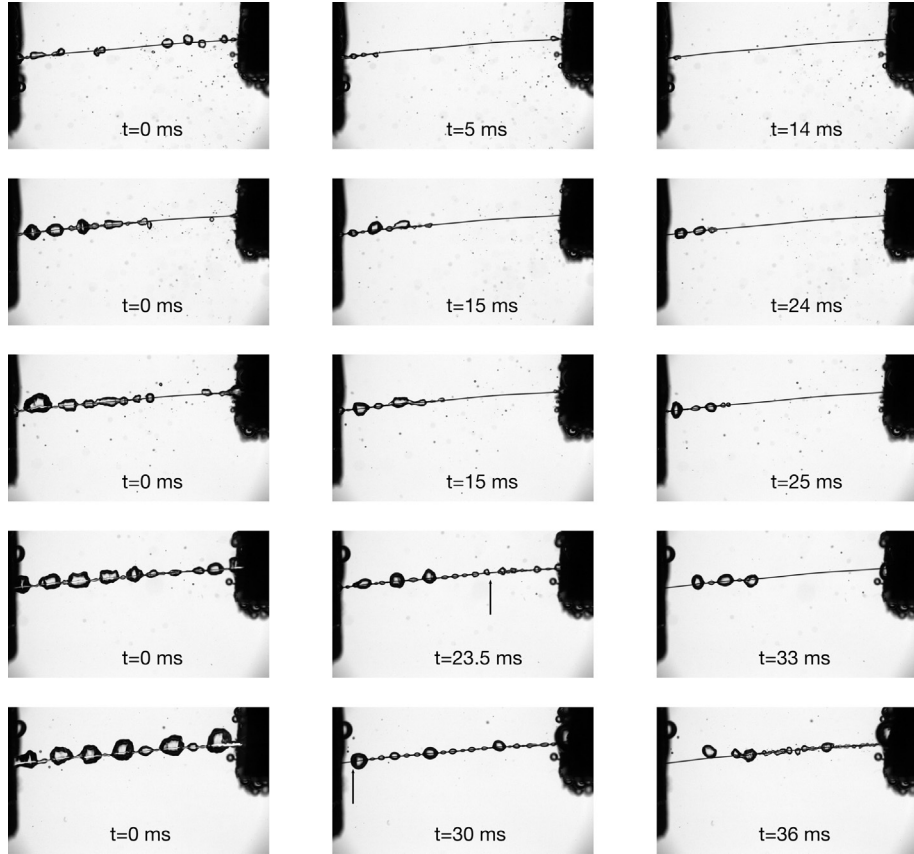


Fig. 12. Photographs of relaxation for tests 6 to 10; each line corresponds to one test; tests are ordered 6–10 and from top to bottom (top = test 6); $t = 0$ corresponds to the end of the pulse; for tests 9 and 10, the arrows point to the initial position of the vapor film end; for test 10, $t = 36$ ms corresponds to breakup collapsing of the film.

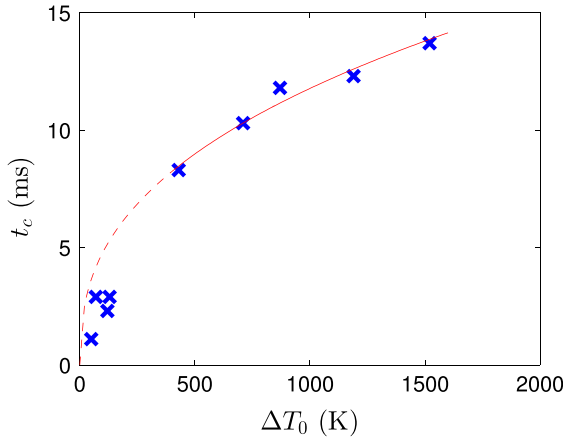


Fig. 13. Characteristic time of temperature relaxation vs. average wire temperature (\times : experimental data; solid/dotted line: power law (Eq. (2))

single-phase convection. It can be suggested that the system follows the boiling curve in the reverse way, as in quenching experiments, with a global transition from film boiling to nucleate boiling when Minimum Heat Flux is reached. At this point, the wire is rewetted and its temperature jumps from the rewetting temperature, T_r , to a temperature close to saturation. This transition is not studied here, and we did not try to measure the corresponding characteristic time. Alternatively, it can happen that the film, instead of breaking homogeneously, enters into a regime of continuous receding up to the size of one bubble, and this without breaking up. This mode of collapse appears less often than the first one, and generally, when a film starts to recede, it is only for a short

time before it breaks up. However, it has been possible to extract from the video recordings, several sequences of rewetting by film receding with a well-defined time evolution. Fig. 15 presents the evolution of the film length with time for two pulses of each test 7 and 8. It is found that the variation of the length is well correlated by $\sim -t^2$. Therefore, the motion of the vapor film edge was characterized by a velocity growing linearly with time, or a constant acceleration in the wire frame.

Analysis of the photographs shows that the edge of the film experiences very locally a sudden transition from film boiling regime to single-phase convection regime. By analogy to homogeneous film break-up scenario, this suggests that, in this case, the boiling curve is run in reverse way through spatial variation (instead of time variation), in a small region close to the edge of the film. It means that the temperature drop between film boiling and single-phase convection is spatially localized. The receding path of the film is thus coincident with the traveling path of a temperature wave along the wire corresponding to the instability of the film boiling regime at zero heat supply similar to transition from nucleate to film boiling studied in [13]. The idea of a transition model from film boiling to single-phase convection controlled by heat conduction in the wire was also postulated by [22].

We modeled then the rewetting phenomenon as a diffusion process, with a nonlinearity in the source term corresponding to a transition at $T = T_r$ between film boiling and single-phase convection (we neglect the nucleate boiling phase). This simple model is considered as sufficient to contain the main physics of the film collapse. In non-dimensional variables, the heat diffusion equation writes

$$\theta_\tau = \theta_{xx} - H(\theta)\theta \quad (3)$$

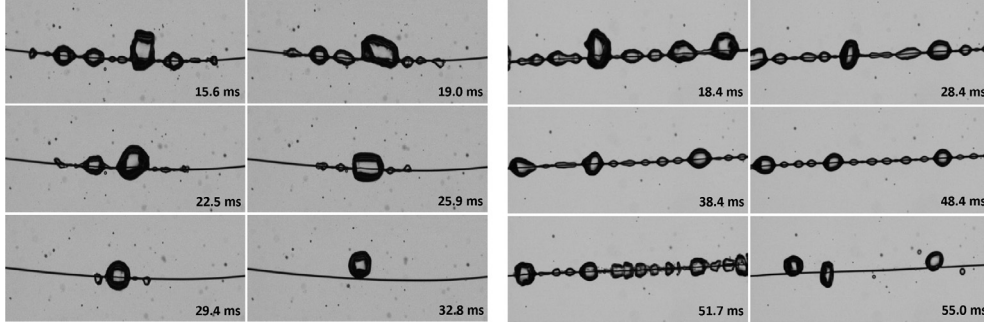


Fig. 14. Modes of film collapse; left: receding film (the Rayleigh-Taylor pattern is maintained but the number of wave periods decreases with time by rewetting of both ends); right: homogeneous break-up (the Rayleigh-Taylor pattern exists up to the instant where vapor production becomes insufficient to sustain the pattern leading to its break-up).

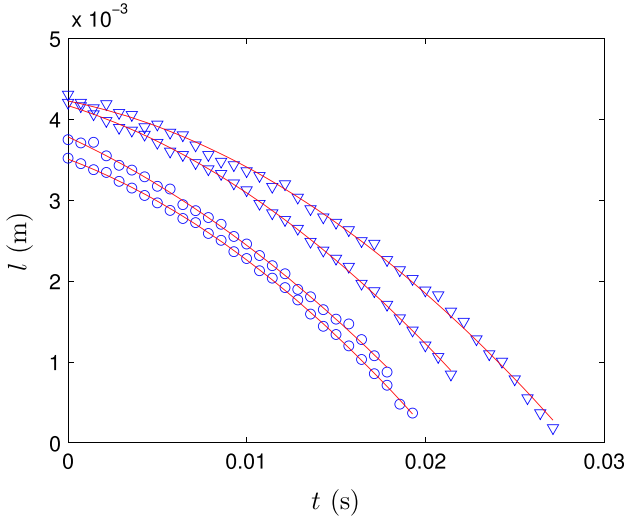


Fig. 15. Film length (l) vs. time for 4 collapsing films; \circ : test 7; ∇ : test 8; solid lines: parabolic fit.

where θ is the superheat scaled by its maximum initial value, H is the non dimensional heat transfer coefficient, $\frac{4hl^2}{k_w D}$, k_w being the thermal conductivity of the wire, X is the position scaled by wire length, and τ , the time scaled by the diffusion time for the characteristic wire length. The H coefficient is H_d in the dry region (film boiling) and H_w in the wetted region (single-phase natural convection). These two regions are separated by the condition $\theta = \theta^*$ located at X^* , where θ^* is the rewetting superheat, ΔT_r , in non-dimensional unit. The boundary conditions are homogeneous Dirichlet at the wetted end and homogeneous Neumann at the dry end. Considering, for simplification, H_d and H_w as constant and independent of temperature, the solution depends only on (X, τ) and two parameters, X_0 the non-dimensional initial length of the vapor film, and θ^* , which is actually depending on the initial temperature of the wire. The numerical solution has been computed for X_0 ranging from 0.2 to 0.8, and θ^* ranging from 0.06 to 0.5 (300 K to 2900 K), conditions that include those of tests 6 to 10. The initial temperature profile is taken as a step function, $\theta = 0$ in the wetted region, and $\theta = 1$ in the dry region. The H values were $H_d \sim 150$ and $H_w \sim 600$, which correspond to the approximate relaxation heat transfer coefficients estimated from the characteristic times of Fig. 13 (the average heat transfer coefficient in relaxation phase, $\rho c R (2t_c)^{-1}$, is 3.4 kW/K/m² for test 7, and 2.8 kW/K/m² for test 8, that is average H is of order 200; $H_w = 600$ is the order of magnitude according to standard

correlation in single-phase convection for an average superheat of 10 K [23] – H_w value characterizes the heat pumping by the wetted region and so has a direct impact on the velocity of the vapor front; with this value, by taking a partition of the wire 3/4 vapor and 1/4 liquid, H_d should be of order 150 to have average heat transfer of order 200; this should explain the chosen values in the results presented below).

Fig. 16 shows the numerical result for one case, where $\tilde{V} = \frac{d\tilde{X}}{d\tilde{\tau}}$, with $\tilde{X} = X^* X_0^{-1}$ and $\tilde{\tau} = \tau \Delta\tau^{-1}$, the time scaled by the time of complete collapse, $\Delta\tau$. It is found that the $X^*(\tau)$ dependence is well approximated by parabola for each (X_0, θ^*) pairs with a minimal r2 value larger than 0.99. This approximation fails at the end of the collapse; in the last instant, the rewetting process accelerates more steeply; however, at this stage, the actual mechanisms are more complex due to capillary effects that become significant, and it is not expected to be physically relevant to consider pure conduction up to the end of the collapse. So, except for this remark, the conduction model gives a good qualitative approximation of the behavior of the experimental film collapse, and we obtain a linear variation of velocity,

$$|\tilde{V}| = K\tilde{\tau}, \quad (4)$$

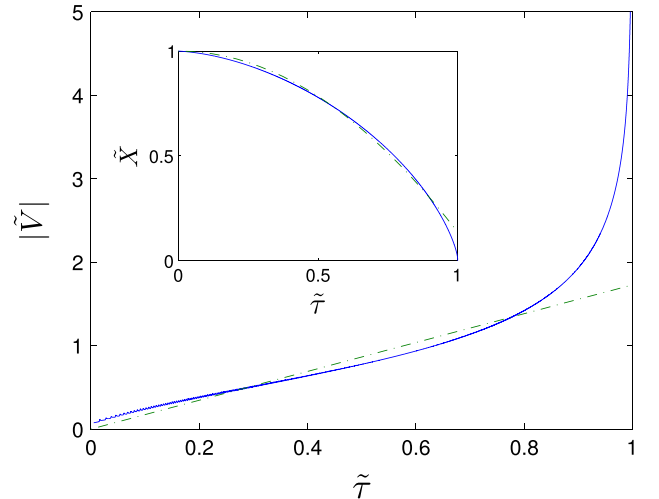


Fig. 16. Velocity of film collapse (\tilde{V}) vs. time; solid line: numerical solution; dotted line: parabolic approximation; $H_d = 150$, $H_w = 600$, $X_0 = 0.273$, $\theta^* = 0.25$ (encapsulated is the corresponding time evolution of film edge position, \tilde{X}).

Fig. 16 shows a comparison between the numerical simulation and the parabolic approximation for $X_0 = 0.273$ and $\theta^* = 0.25$ ($\Delta T_0 \approx 1100$ K).

A comparison of the conduction model with the experimental data is proposed in Fig. 17. It must be stressed that the exact values for the controlled parameter (initial wire temperature in dry region, heat transfer coefficients, initial length to be taken), are not known and the initial conditions for the film collapse cannot be deduced from the experimental data. Fig. 17 gives the acceleration of the parabolic approximation, a_0 (m/s^2), vs. the initial length, with the initial wire superheat in the dry region as a parameter (heat transfer coefficients are here kept constant); for the numerical solution, this acceleration is related to the non-dimensional collapsing acceleration (i.e. the second time derivative of the film length), K , by a scaling factor equal to $\alpha_w^2 X_0 (L^3 \Delta \tau^2)^{-1}$, α_w being the heat diffusion coefficient of tungsten. For tests 7 and 8, the initial average superheat are 693 K and 858 K (Fig. 11); if we assume zero superheat in the wetted region, the average temperature in the dry region should be of order 2000 K. For test 9, the same rule of thumb gives an estimated value of 220 K, and for test 10, around 190 K. It can be thus observed that, even if the values between experiment and model differ significantly, the experimental data have a similar variation as the conduction model for the initial wire temperature effect. The qualitative agreement between the model and the experimental data (constant acceleration, effect of initial temperature) shows that the film collapse may be partly governed by a temperature traveling wave. The presence of unknown input parameters in the model has the main drawback that it cannot enable one to estimate experimentally one of this parameter (for instance the rewetting temperature). An interesting point is that the position of the film edge versus time is close to a unique curve for the considered values of heat transfer coefficients. It means that in non dimensional variables, the solution can be obtained as a simple geometrical transformation of a unique shape function, $\tilde{X} = 1 - K\tilde{\tau}^2$, with $K = K(X_0, \theta^*)$, the acceleration, H_d and H_w being fixed. The wave solution depends on the magnitude of this two parameters. H_w influences the velocity of the wave front and H_d the cooling rate of the dry region. The experimental apparition of this mode of collapse necessitates that these two parameters are well matched. For instance, in test 10, the wire temperature is close to the rewetting temperature at the beginning of the collapse, and the receding film regime rapidly stops and film break-up takes place (Fig. 12).

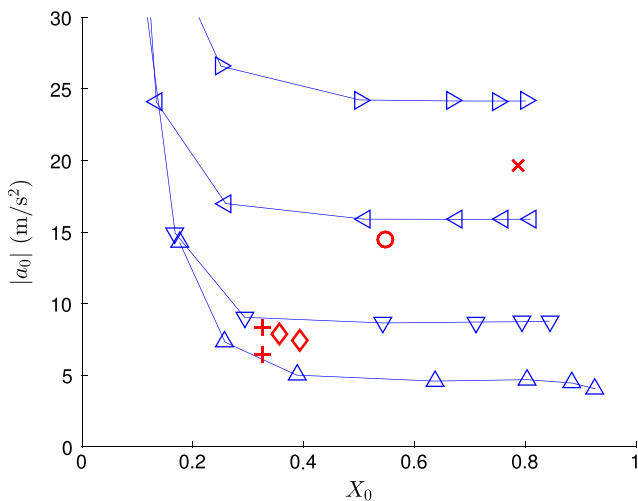


Fig. 17. Acceleration of film edge in parabolic collapse as function of initial length and initial superheat of dry region; \triangle : $\Delta T_0 = 1720$ K; ∇ : $\Delta T_0 = 688$ K; \triangleleft : $\Delta T_0 = 430$ K; \triangleright : $\Delta T_0 = 344$ K; +: test 7; \diamond : test 8; \circ : test 9; \times : test 10.

4. Conclusion

Pulse boiling experiments on a thin wire heater were conducted. Average quantities such as heat flux and wire temperature were measured and rapid video (14,000 fps) of transient boiling were recorded. Both heating and relaxation were analyzed. The heat transfer during heating is different at low and high heat supply with a threshold of order $UI \sim 15$ W or heating rate $dT/dt \sim 3 \times 10^5$ K/s. For large power supply, the transition to film boiling occurs in the way of an explosive vapor wave initiated at one large bubble. This transition is characterized by a certain amount of energy input in the wire and a sudden change in the slope of the time evolution of wire temperature, $T_w(t)$. For the largest heat supply used, this transition occurs before nucleate boiling sets up, which shows how this mechanism is not related to classical CHF. For lower power supply, we find the same behavior as for steady boiling, i.e. transition from nucleate boiling to film boiling by a mechanism of bubble coalescence (i.e. limit of vapor production by isolated bubbles). After this transition, in all cases, the heat transfer relaxes towards a unique curve in film boiling regime that corresponds to values of heat transfer coefficient by an order of magnitude larger than in case of steady boiling. During relaxation, two modes of vapor film collapse have been found. The first mode has been identified to homogeneous vapor film break up, and the second as a receding film mechanism. This second mode has been approached with qualitative agreement by a wire temperature autowave process modeled on the basis of 1D heat diffusion in the wire with a two values non linear heat transfer coefficient. However, the proper modeling of those different situations is far from being solved, and remains difficult due to the role of heterogeneities in the different field quantities and in the mechanisms of heat transfer. It seems to the authors that further investigations should account for the instability phenomena outlined in this study, and more particularly, for the heat conduction in the heating medium.

Acknowledgement

The authors acknowledge Sébastien Cazin, Hervé Ayroles and Grégory Ehses at IMFT, Toulouse, for their technical assistance.

References

- [1] H. Auracher, W. Marquardt, Experimental studies of boiling mechanisms in all boiling regimes under steady-state and transient conditions, *Int. J. Therm. Sci.* 41 (7) (2002) 586–598.
- [2] R. Visentini, C. Colin, P. Ruyer, Experimental investigation of heat transfer in transient boiling, *Exp. Therm. Fluid Sci.* 55 (2014) 95–105.
- [3] Y. Katto, H. Ohno, An improved version of the generalized correlation of critical heat flux for the forced convective boiling in uniformly heated vertical tubes, *Int. J. Heat Mass Transfer* 27 (9) (1984) 1641–1648.
- [4] A. Sakurai, M. Shiotsu, K. Hata, A general correlation for pool boiling heat transfer from a horizontal cylinder to subcooled liquid, *J. Heat Transfer* 112 (1990) 430–440.
- [5] V.P. Skripov, *Metastable Liquids*, John Wiley and Sons, 1974.
- [6] K.P. Derewnicki, Experimental studies of heat transfer and vapour formation in fast transient boiling, *Int. J. Heat Mass Transfer* 28 (1985) 2085–2092.
- [7] D.N. Sinha, L.C. Brodie, J.S. Semura, Liquid-to-vapor homogeneous nucleation in liquid nitrogen, *Phys. Rev. B* 36 (1987) 4082–4085.
- [8] S. Glod, D. Poulikalos, Z. Zhao, G. Yadigaroglu, An investigation of microscale explosive vaporization of water on an ultrathin pt wire, *Int. J. Heat Mass Transfer* 45 (2002) 367–379.
- [9] Y. Iida, K. Okuyama, K. Sakurai, Boiling nucleation on a very small film heater subjected to extremely rapid heating, *Int. J. Heat Mass Transfer* 37 (1994) 2771–2780.
- [10] G. Berthoud, L. Gros d'Aillon, Film boiling heat transfer around a very high temperature thin wire immersed into water at pressure from 1 to 210 bar: experimental results and analysis, *Int. J. Therm. Sci.* 48 (2009) 1728–1740.
- [11] J.D. Bernardin, I. Mudawar, The leidenfrost point: experimental study and assessment of existing models, *J. Heat Transfer* 121 (1999) 894–903.
- [12] N. Bakhru, J.H. Lienhard, Boiling from small cylinders, *Int. J. Heat Mass Transfer* 15 (1972) 2011–2025.

- [13] S.A. Zhukov, V.V. Barelko, A.G. Merzhanov, Wave processes on heat generating surfaces in pool boiling, *Int. J. Heat Mass Transfer* 24 (1980) 47–55.
- [14] V.I. Krinsky (Ed.), *Self-Organization Autowaves and Structures Far from Equilibrium*, Springer-Verlag, Berlin, 1984.
- [15] H.A. Jones, A temperature scale for tungsten, *Phys. Rev.* 28 (1926) 202–207.
- [16] Y. Kraftmakher, High-temperature specific heat of metals, *Eur. J. Phys.* 15 (1994) 329–334.
- [17] W.M. Rohsenow, A method of correlating heat transfer data for surface boiling of liquid, *J. Heat Transfer* 74 (1952) 969–976.
- [18] A.L. Bromley, Heat transfer in stable film boiling, *Chem. Eng. Prog.* 46 (5) (1950) 221–228.
- [19] J.H. Lienhard, V.K. Dhir, Hydrodynamic prediction of peak pool-boiling heat fluxes from finite bodies, *J. Heat Transfer* 95 (2) (1973) 152–158.
- [20] P. Spiegler, J. Hopenfeld, M. Silberberg, C.F. Bumpus Jr., A. Norman, Onset of stable film boiling and the foam limit, *Int. J. Heat Mass Transfer* 6 (1963) 987–994.
- [21] A. Sakurai, M. Shiotsu, K. Hata, K. Fukuda, Photographic study on transitions from non-boiling and nucleate boiling regime to film boiling due to increasing heat inputs in liquid nitrogen and water, *Nucl. Eng. Des.* 200 (2000) 39–54.
- [22] H. Ohtake, Y. Koizumi, Study on propagative collapse of a vapor film in film boiling, *Int. J. Heat Mass Transfer* 47 (2004) 1965–1977.
- [23] V. Morgan, The overall convective heat transfer from smooth circular cylinders, *Adv. Heat Transfer* 11 (1975) 199–264.